

Lithium Adsorption on Graphene at Finite Temperature

Yusuf Shaidu,^{†,‡} Emine Kucukbenli,[‡] and Stefano de Gironcoli^{*,‡}

[†]*The Abdus Salam International Centre for Theoretical Physics, Trieste, Italy*

[‡]*International School for Advanced Studies, Trieste, Italy*

E-mail: degironc@sissa.it

Effect of periodic boundary conditions along the aperiodic direction

Here we give a brief analysis of the effect of periodic boundary conditions (PBC) on energetics reported in the main article. In our calculations, the vacuum size between adjacent graphene sheets is set to 20 Å. To demonstrate the impact of this parameter on the adsorption energy, we perform Li adatom adsorption calculations on a 3x3 graphene supercell while varying the vacuum size, i.e. graphene layer separation (LS) between 10 and 30 Å. The single Li adatom on graphene case has the highest amount of charge transfer, therefore, it is expected to have the most pronounced long-range electrostatic behaviour between graphene sheets. Hence the error reported here can be seen as an upper bound to the impact of PBC.

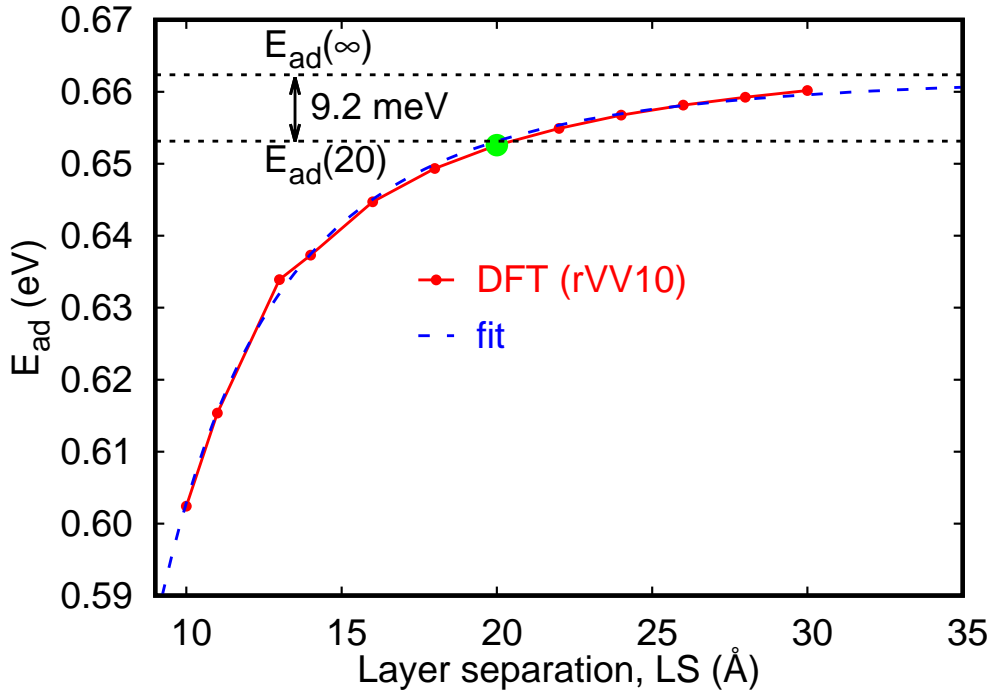


Figure S1: Adsorption energy(E_{ad}) of Li adatom on the hollow site of 3x3 graphene supercell as a function layer separation (LS). The infinite layer separation limit, $E_{ad}(\infty)$ was obtained via fitting using Eq.1. The parameters of the fit are $E_{ad}(\infty) = 0.662362$, $b = -3.04981$; $c = 3.05586$. R is the nearest neighbor distance for Li in-plane, $R = 3 \times 2.47$ Å in the case of 3x3 supercell. The root-mean-square (rms) error of the fit is 0.77 meV.

Fig. S1 shows the adsorption energy, E_{ad} referenced to bulk Li as a function of layer

separation (LS). In order to estimate the adsorption energy at infinite separation, we fit the DFT data (red curve of Fig. S1) to a simple function of LS and the in-plane distance between Li adatoms on surface, R:

$$E(LS) = E_{ad}(\infty) + \frac{b}{LS} + \frac{c}{\sqrt{(R^2 + LS^2)}} \quad (1)$$

This functional form mimics the Coulomb interaction of Li adatom and its periodic images on adjacent graphene layers, as well as the interaction with the periodic images of its nearest neighbors. Therefore at infinite layer separation, we can approximate the energy as $E_{ad}(\infty)$. The difference in adsorption energy between $LS=\infty$ and $LS=20 \text{ \AA}$ is estimated to be 9.2 meV. This value is smaller than the energy difference between Li-adatom and Li-cluster phases at 0K (which ranges between 44 and 176 meV on a 3x3 supercell and between 149 and 312 meV on a 6x6 supercell). Therefore the results calculated at $LS=20 \text{ \AA}$ can be considered as a good approximation to the infinite separation limit for the analysis of phase stability at 0 K.

We can confirm this by observing the electronic density profile as well: The planar average of the charge density difference in Fig. S2 shows that the charge density profile does not change significantly at layer separations above 16 \AA .

The impact of PBC on the model that is used in finite temperature study can be analyzed as follows: The cluster expansion interaction potential is obtained via a fit to DFT energies. The standard deviation of this fit is 18.0 meV, while the upper-bound of the correction due to PBC is estimated to be ≈ 9 meV using the fit demonstrated above. Thus, the results calculated at $LS=20 \text{ \AA}$ can be considered as a good approximation to the infinite separation limit for the analysis of phase stability also at finite temperatures.

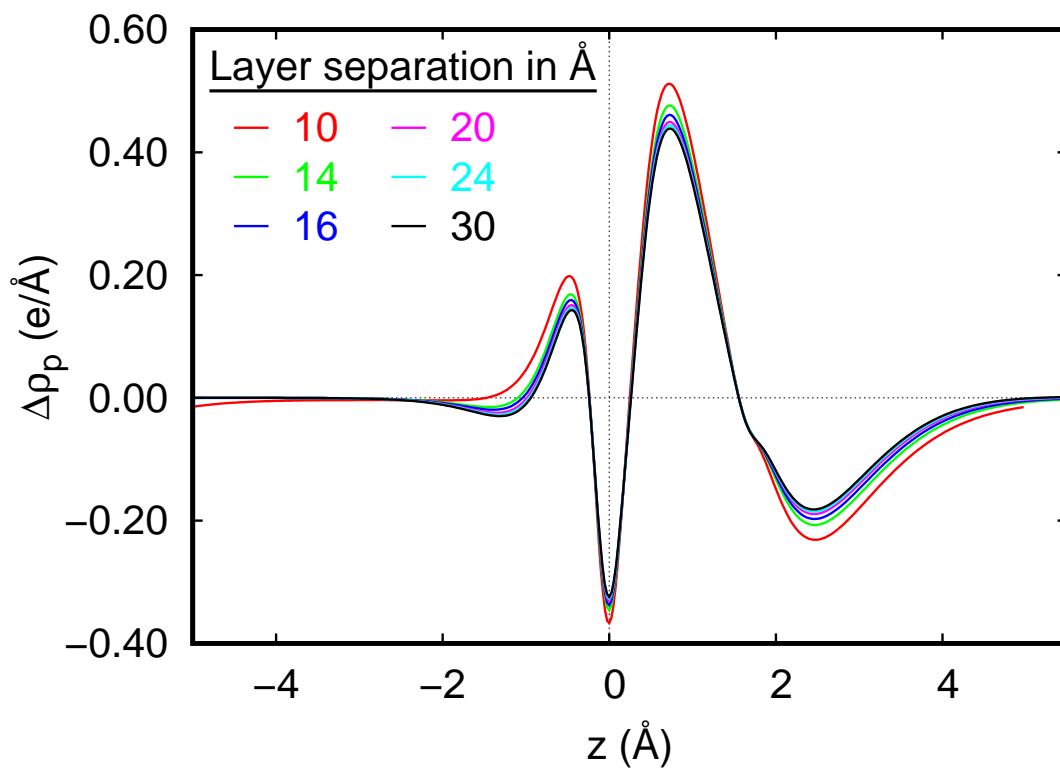


Figure S2: The planar average of the charge density difference between pristine graphene and Li-adsorbed graphene, $\Delta\rho_p(z) = \int \Delta\rho(x, y, z) dx dy$, plotted at different graphene layer separations as a function of the perpendicular distance from the graphene plane (situated at $z = 0$ Å)

Fitting procedure

The performance of the Cluster Expansion model was optimized by minimizing the standard deviation, σ , of the adsorption energies predicted by the model from the adsorption energies obtained by density functional theory (DFT). In order to avoid overfitting and favor locality, a penalty term to the cost function was added. The penalty matrix was defined so that the two body interactions are penalized proportionally to the distance of the interacting pairs; for instance, the element for second nearest neighbor interaction is multiplied by $(\sqrt{3.0})^\lambda$. This imposed locality constraints to the 2-body terms similar to the one developed in Ref. 1. The total cost function per Li is defined as

$$\sigma_{Li}^2 = \frac{1}{N_{config}} \sum_{i=1}^{N_{config}} \left[\frac{E_{DFT}^i - E_{CE}^i}{N_{Li}} \right]^2 + t \sum_{i=1}^{N_J} J_i M_i J_i, \quad (2)$$

where the accuracy of the model is defined as

$$\sigma_{Li}^2 = \frac{1}{N_{config}} \sum_{i=1}^{N_{config}} \left[\frac{E_{DFT}^i - E_{CE}^i}{N_{Li}} \right]^2 = \frac{1}{N_{config}} \sum_{i=1}^{N_{config}} \sigma_i^2, \quad (3)$$

and σ_i^2 is the square deviation per Li of the model adsorption energy of configuration i from DFT one.

Similarly, the mean square deviation per carbon is given by

$$\sigma_C^2 = \frac{1}{N_{config}} \sum_{i=1}^{N_{config}} \left(\frac{N_{Li}}{N_C} \right)^2 \sigma_i^2. \quad (4)$$

In matrix form the cluster expansion for a given configuration C is given by

$$E_{CE}(C) = \sum_f J_f \Pi_f(C) \quad (5)$$

and the cost function per Li atom is given by

$$\sigma_{Li}^2 = \frac{1}{N_{config}} \sum_C (E_{DFT} - \Pi J)^T (E_{DFT} - \Pi J) + t J^T M J. \quad (6)$$

Here, M is a diagonal matrix with elements that depend on the range of J for 2-body interactions and 1.0 otherwise. We used $t = 0.0005$ and $\lambda = 1.0$. Thus, the extra cost associated with the locality constraint is minimal and only play a significant role when less configurations than parameters are fitted.

Fitted configurations

The fitted configurations are Li-atom in 2x2 to 8x8 supercell, Li-dimer in 3x3 to 7x7 supercells, Li-trimer in 3x3 to 7x7 supercells and Li-tetramer in 3x3 to 6x6 supercells, the 5- and 6-Li atom clusters in the 4x4 supercell of graphene and those shown in Fig. S3 which are mixture of clusters and adatoms.

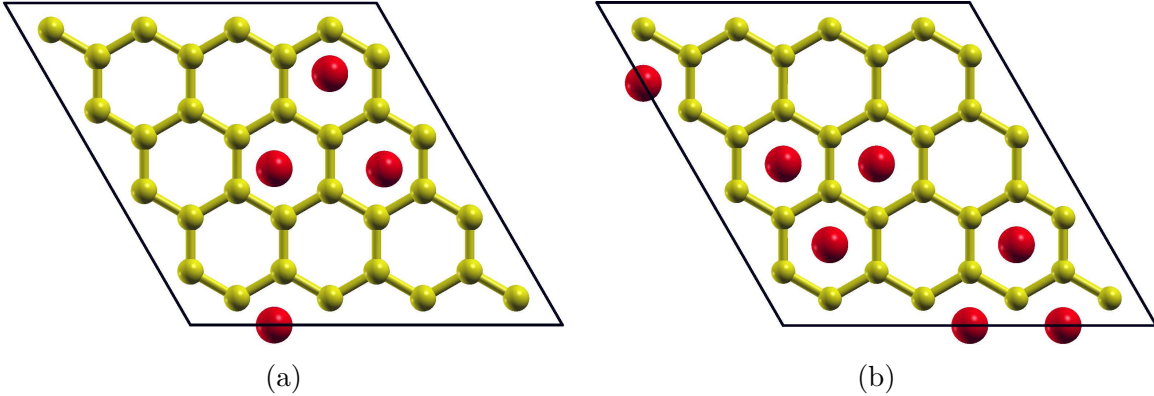


Figure S3: A pair of generic Li atom configurations in a 4x4 graphene supercell with (a) 4 Li atoms per unit cell and (b) 7 Li atoms per unit cell.

Monitoring the fitting procedure

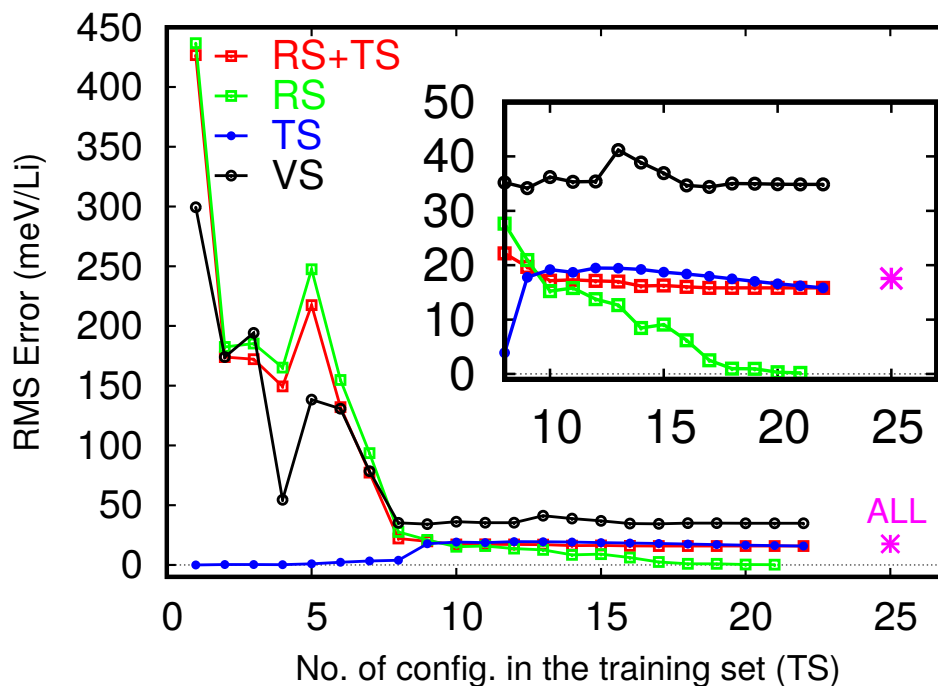


Figure S4: Evolution of the root-mean-square (RMS) error as the number of configurations used in fitting, i.e. in the training set (TS), increases. In this analysis, we use a total of 25 different configurations of Li on graphene. Three configurations are set aside as validation set (VS) and are never included during the training of the model. Therefore, at zeroth step of the training, we have zero configurations in the training set (TS) and 22 configurations in the remaining set (RS). At each step of the training the configuration with the largest prediction error is added to TS, reducing the number of configurations in the RS by one. We continue these training steps until all 22 configurations in RS have been added to TS. Finally, for analysis purposes we also perform a training including all 25 configurations (magenta asterisk labeled as ALL). The inset shows the zoom of the plot at later steps of training where RMS error converges for TS.

Performance of the model

In Fig. S5 the deviation of the DFT energy from the energy predicted by the full model described in the manuscript is shown. The root-mean-square deviation is 18.0 meV/Li (1.6 meV/C) with a cross validation error of 30.2 meV/Li (3.2 meV/C) as already reported in the main text.

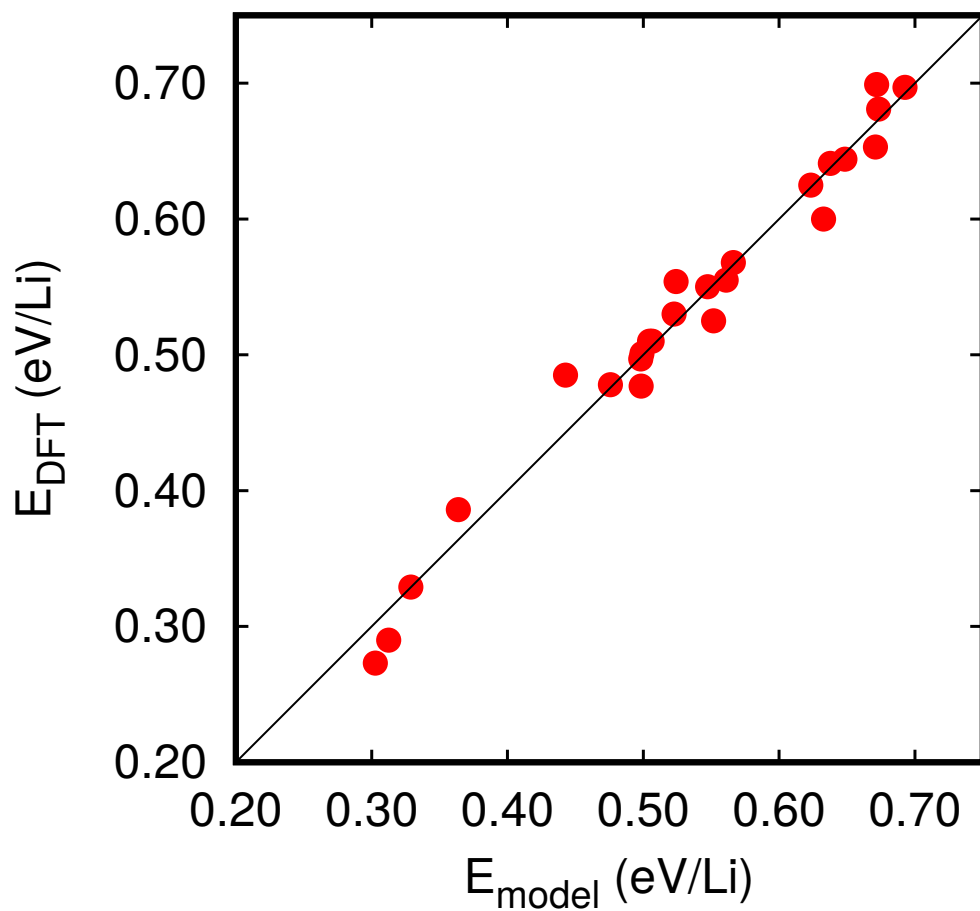


Figure S5: Comparison of the model energies with DFT ones using rVV10 functional. The black line represents perfect agreement while the red points are the actual model predictions.

Table S1: Best fit values for the effective cluster interactions of the model when 3- and 4-body interaction terms are neglected. All parameters, except γ , in eV.

	J_1	J_{2a}	J_{2b}	J_{2c}	J_3	J_4	J_{dd}	γ
ECI	0.429	0.074	-0.177	0.051	0.000	0.000	1.198	0.559

When 3- and 4-body terms are neglected, the obtained results are similar to the one reported in Ref. 2: the most influential cluster figure is the point cluster as shown in table S1. The resulting root-mean-square deviation is 98.3 meV/Li (7.5 meV/C) with a cross validation error of 158.2 meV/Li (21.2 meV/C). The reduced quality of the model is shown in Fig. S6.

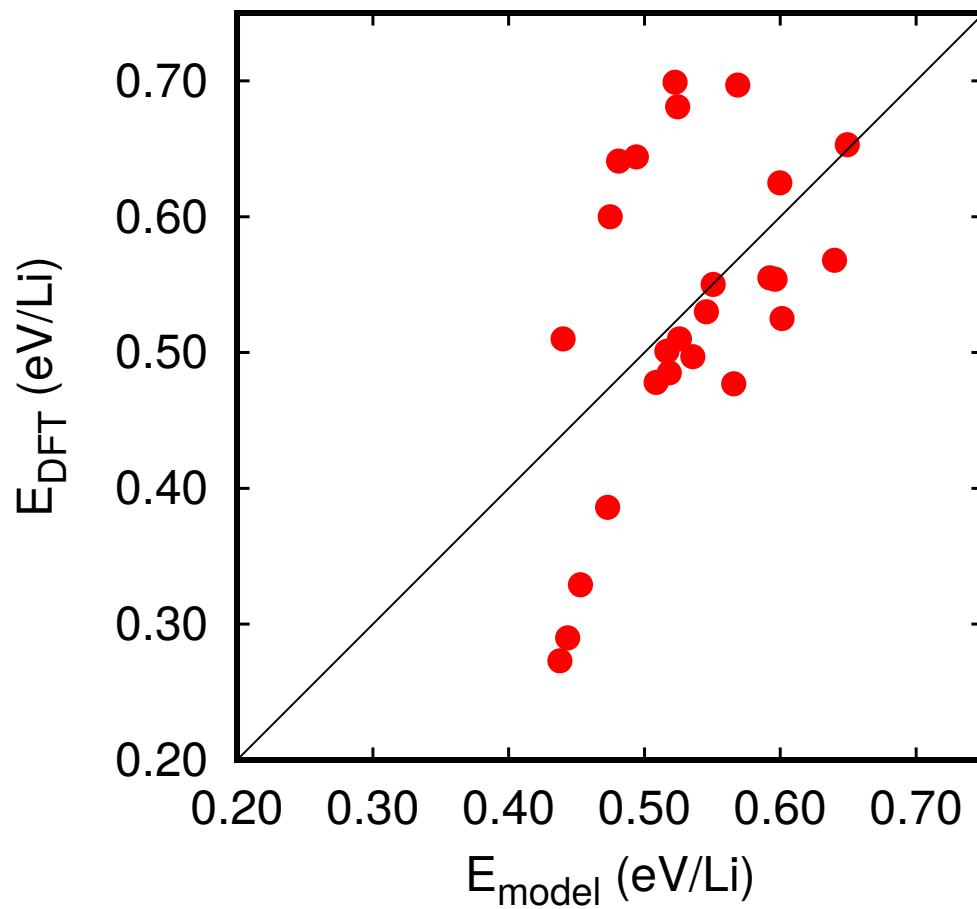


Figure S6: Comparison of the model energies with DFT ones using rVV10 functional when 3- and 4-body interaction terms are neglected. The black line represents perfect agreement while the red points are the actual model predictions.

Even less accurate results are obtained when in addition, the J_{dd} term is set to zero. Results are reported in table S2. The root-mean-square deviation is 108.3 meV/Li (7.3 meV/C) with a cross validation error of 133.9 meV/Li (15.3 meV/C). The DFT *vs* model comparison is shown in Fig. S7. This is a strong indication that the long-range dipole-dipole term and the 3- and 4- body interactions are very important for a proper description of Li adsorption on graphene.

Table S2: Best fit values for the effective cluster interactions of the model when 3- and 4-body and long-range interaction terms are neglected. All parameters, except γ , in eV

	J_1	J_{2a}	J_{2b}	J_{2c}	J_3	J_4	J_{dd}	γ
ECI	0.486	0.068	-0.077	0.045	0.000	0.000	0.0000	0.000

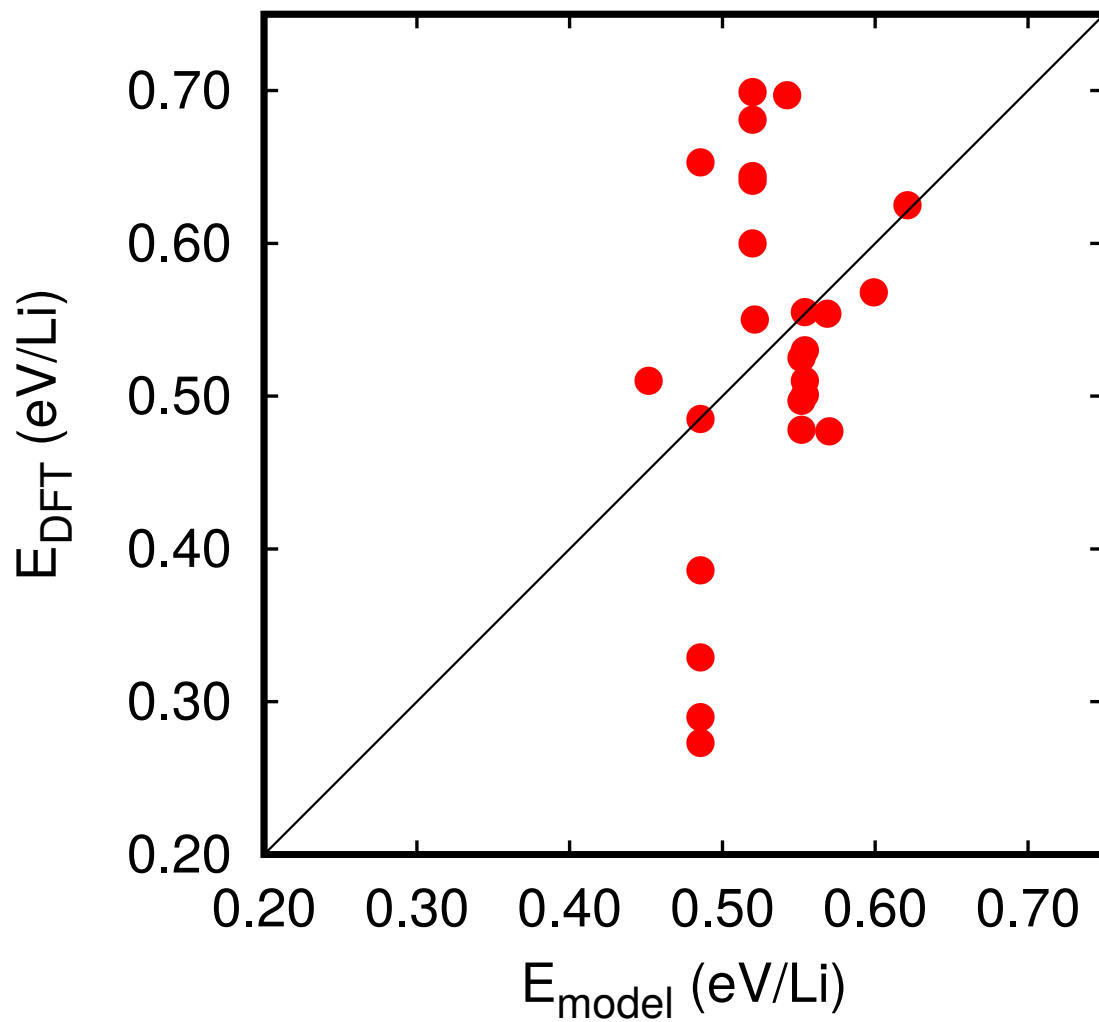


Figure S7: Comparison of the model energies with DFT ones using rVV10 functional when 3- and 4-body and long-range interaction terms are neglected. The black line represents perfect agreement while the red points are the actual model predictions.

When only the dipole-dipole long-range terms are neglected the resulting parameters are the ones reported in table S3 (DFT *vs* model deviations shown in Fig. S8). This model describes relatively well the Li-dense configurations, but dilute configurations with Li adatoms in 3x3 to 8x8 are poorly described indicating the importance of the long-range dipole-dipole interaction term.

The root-mean-square deviation is 70.9 meV/Li (5.2 meV/C) with a cross validation error of 91.9 meV/Li (8.6 meV/C)

Table S3: Best fit values for the effective cluster interactions of the model when only the dipole-dipole long-range terms are neglected. All parameters, except γ , in eV

	J_1	J_{2a}	J_{2b}	J_{2c}	J_3	J_4	J_{dd}	γ
ECI	0.408	0.491	-0.037	0.065	-1.130	0.196	0.0000	0.000

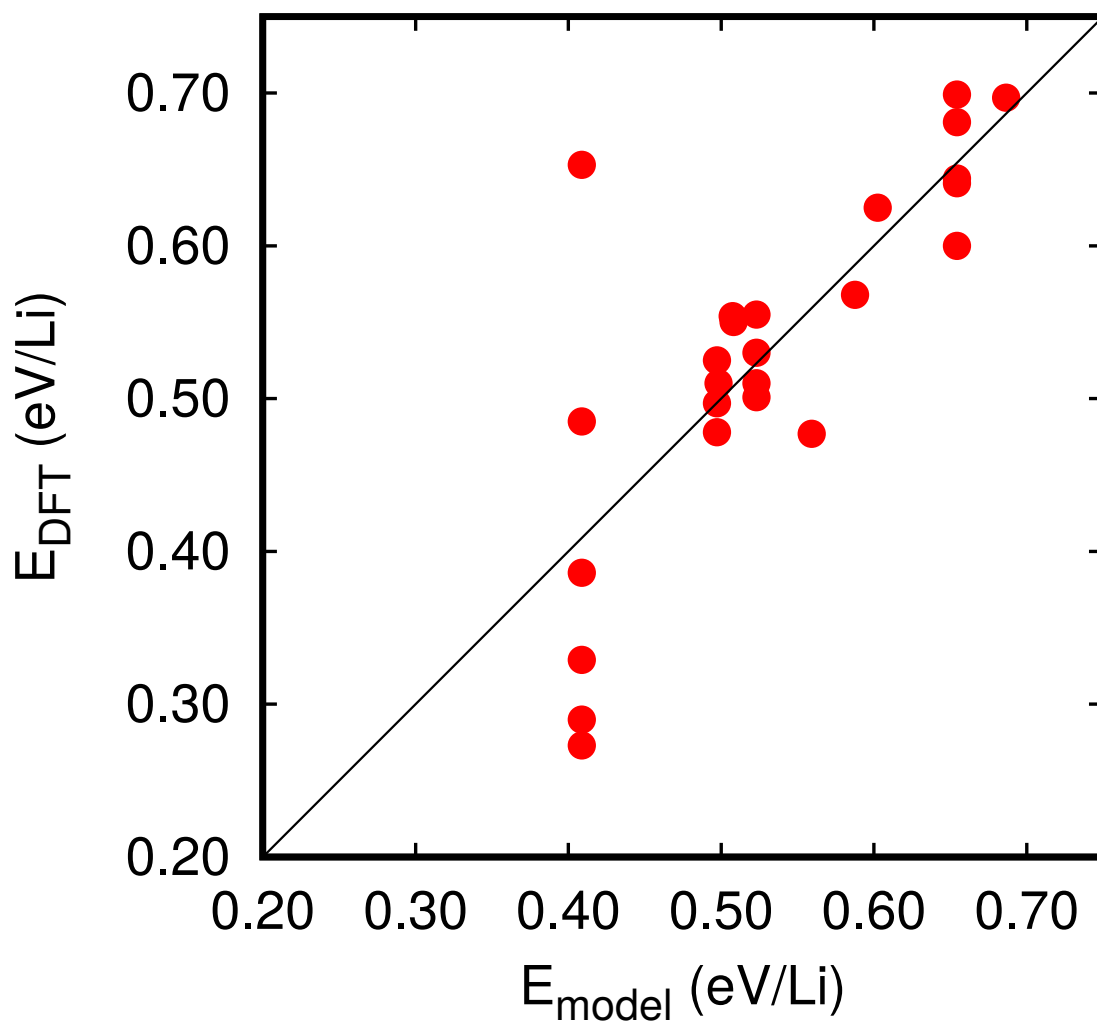


Figure S8: Comparison of the model energies with DFT ones using rVV10 functional when only the long-range interaction terms are neglected. The black line represents perfect agreement while the red points are the actual model predictions.

Cluster Expansion : The behaviour of the dipole-dipole interaction term

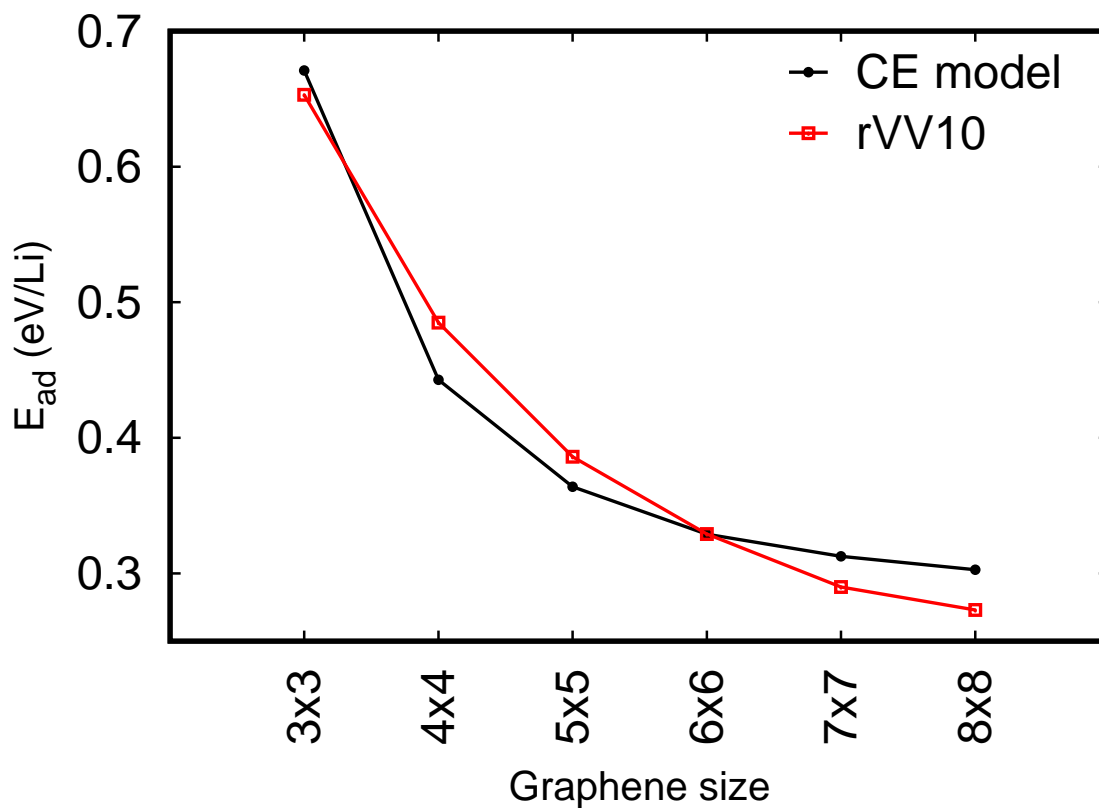


Figure S9: The behaviour of the dipole-dipole part of the cluster expansion model obtained via single Li adatom on various supercell sizes. Note that in all the supercell sizes used, Li ions in adjacent cells are far enough that the only contributions to the model energy are the onsite term, which constitutes a constant shift, and the long-range interaction term. The model can be seen to capture the long-range behaviour observed in the DFT calculations (red squares)

Finite size analysis

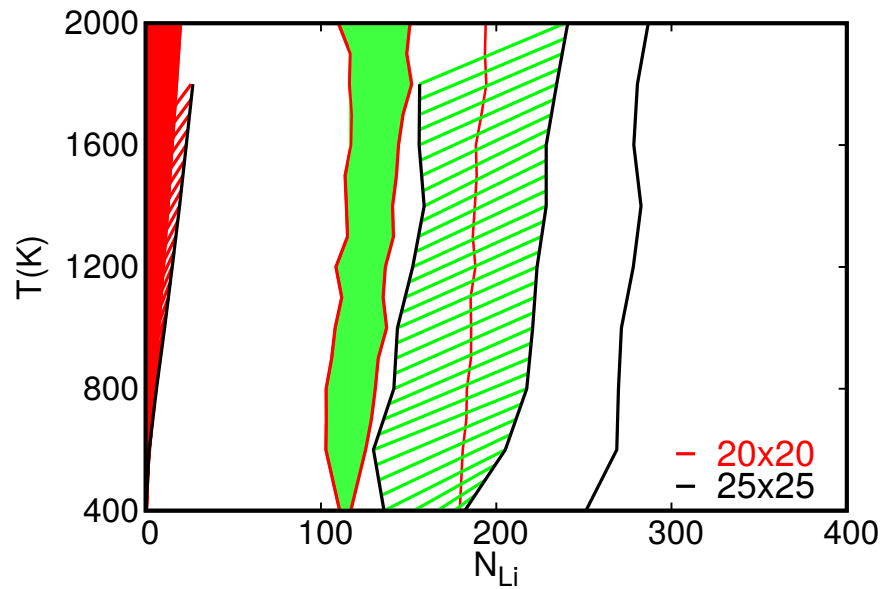


Figure S10: Finite size effects: Temperature versus number of Li N_{Li} phase diagram. The red lines represent the phase boundaries determined with a 20x20 supercell and the black lines represent those determined with the 25x25 supercell. The red and green shaded region are the Li-gas and Li-island phases in a 20x20 cell while the red and green hatch regions are corresponds to those obtained with 25x25 supercell. The plot shows the increased dimension of the Li-islands in equilibrium with the Li-stripe phase as a function of the simulation box size.

References

- (1) Laks, D. B.; Ferreira, L. G.; Froyen, S.; Zunger, A. Efficient Cluster Expansion for Substitutional Systems. *Phys. Rev. B* **1992**, *46*, 12587–12605.
- (2) Lee, E.; Persson, K. A. Li Absorption and Intercalation in Single Layer Graphene and Few Layer Graphene by First Principles. *Nano Lett.* **2012**, *12*, 4624–4628.